 

https://doi.org/10.1070/QEL17301

# Effect of the magnetic field on the size of nanoparticles obtained by ablation of a cobalt–copper target in a liquid

Yu.S. Tveryanovich, G.O. Abdrashitov, L.G. Menchikov

*Abstract.* **Co–Cu nanoparticles were obtained by pulsed laser ablation in a liquid medium in a constant magnetic field. The organic solvent, hexane, served as a liquid medium. The influence of the magnetic field on the formation of nanoparticles was studied. It is shown that the magnetic field leads to a decrease in the size distribution width of the resulting nanoparticles.**

***Keywords:*** *nanoparticles, cobalt, laser ablation, magnetic field.*

## 1. Introduction

The development of modern heterogeneous catalysis is directly related to the development of nanotechnology in general and precision methods for the synthesis of nanomaterials in particular. Intermetallic nanoobjects occupy a significant place in catalysis.

The modern approach to the creation of metallic nanostructured materials consists in growing metal nanoparticles, nanowhiskers and nanofilms from solutions [1–3], as well as by the methods of vacuum epitaxy [4, 5] and plasma spraying [6]. None of these methods is free from disadvantages. Some of them require the use of various reagents and are accompanied by co-products, often with significant toxicity. Others require bulky and expensive vacuum technology. Still others have a low yield of the target product, which leads to high final cost of the product [7].

The advantages of the method of laser ablation in liquid are its versatility, possibility of using a wide range of materials, ease of implementation, as well as the absence of the need for vacuum technology and the need for reagents, especially in cases where ablation is carried out in water. In Refs [8–10], the applicability of the method for ablation of pure metals, as well as copper containing alloys of complex composition (bronze, brass), is considered. Kazakevich et al. [8] showed the possibility of self-ordering of the target surface depending on the parameters of laser radiation, which makes it possible to use not only the nanoparticles obtained, but also the activated target as catalysts. Goncharova et al. [10] found that the use of alcohol as a liquid medium for laser ablation of copper leads to the formation of predominantly metallic nanoparticles. However, this method is not free from disadvantages, too. Like other methods of deep dispersion, it does not allow sufficiently accurate setting the size of the resulting nanoparticles, and hence their specific surface area, which causes a significant decrease in the catalytic properties of the target product [11].

Cobalt-based nanoparticles have significant catalytic activity [12, 13], which can be substantially increased by introducing other metals as a modifier [14]. Based on the literature data [15–17], we chose copper. It should be borne in mind that not only pure cobalt nanoparticles but also copper–cobalt nanoparticles have ferromagnetic properties [18]. Ferromagnetism with a coercive field of 0.036 T was found for nanoparticles, the copper content of which exceeded the cobalt content by 1.4 times. According to the authors' data, nanoparticles obtained by joint implantation of metals into a quartz glass matrix had the structure of solid solutions with a face-centred cubic lattice. The same structure was observed for ferromagnetic nanocrystals formed in a multilayer film on a silicon substrate with cobalt layers 1.9–2.0 nm thick and copper layers 0.5–1.3 nm thick [19].

In this work, an attempt is made to improve the controllability of the synthesis of heterometallic Co–Cu nanoparticles by laser ablation in a liquid using a target with a given morphology as a result of exposure to a magnetic field.

## 2. Experimental technique

Bimetallic targets of the cobalt–copper composition were prepared by the method of ion sputtering on the surface of polished high-purity nickel. For deposition, we used a Gatan PECS 682 system with an accelerating voltage of 30 keV, which makes it possible to obtain layers with a thickness of 0.1 nm. The bombardment of cobalt and copper was carried out with argon ions. As sources of cobalt and copper, we used samples of epitaxial-quality single crystals (99.99% purity).

An Amplitude Technology laser complex with a wavelength of 795 nm, a pulse repetition rate of 50 Hz, and a pulse energy of 1.45 mJ was used for ablation. The pulse duration was 2 ps. Ablation was performed in the focus of an optical system with a focal length of 100 mm. The focal spot diameter was 300 μm. Thus, the energy density of the radiation pulse was 15 mJ mm$^{-2}$, and the power density was 15 GW mm$^{-2}$.

Ablation was implemented in a liquid medium (reagent grade hexane) with preliminary purging with argon for 20 min to remove dissolved oxygen. The sample volume was 1.2–1.45 mL. The ablation time was 15 min.

Nanoparticles obtained by ablation were removed from the solution by centrifugation at an acceleration of 8000 g. Then the extracted particles were deposited on a prepared

**Yu.S. Tveryanovich, G.O. Abdrashitov** Institute of Chemistry, Saint-Petersburg State University, Universitetskii prosp. 26, 198504 St. Petersburg, Russia; e-mail: georgy.vg@gmail.com;
**L.G. Menchikov** Zelinsky Institute of Organic Chemistry, Russian Academy of Sciences, Leninsky prosp. 47, 119991 Moscow, Russia

Received 20 February 2020
*Kvantovaya Elektronika* **50** (9) 861–865 (2020)
Translated by V.L. Derbov

silicon plate to obtain their images by scanning electron microscopy and conduct elemental analysis of the sample.

To study the morphology and dimensional parameters of nanoparticles, a Zeiss Supra 40VP scanning electron microscope with a maximum magnification of 2 nm was used. The microscope was equipped with an attachment for elemental analysis of samples.

When studying the effect of a magnetic field on the ablation of a cobalt–copper target, we used a permanent neodymium magnet made of NdFeB, grade N35H, in the form of a cylinder 19 mm in diameter and 4 mm high, which created a magnetic field in the quartz cell with a magnetic induction of ~890 G. In Ref. [20], a similar technique was used to collect nanoparticles during laser ablation of a cobalt-based alloy in an argon jet.

## 3. Results and discussion

### 3.1. Target fabrication

The cobalt–copper phase diagram is a peritectic-type diagram with limited solubility of metals in each other (up to 5% cobalt in copper and up to 7.3% copper in cobalt). According to some data [8, 21, 22], nanoparticles with the limiting solubility of up to 18% for both alloy components were obtained by the methods of sol–gel growth followed by annealing in an inert gas flow, as well as by the method of laser ablation. The catalytic properties of Co–Cu nanoparticles are due to the contact of at least two different phases: solid solutions based on cobalt and based on copper. Therefore, to obtain such nanoparticles, their gross composition must sufficiently differ from the compositions of both solid solutions. Based on this, the following ratio of the gross content of cobalt and copper was chosen: [Cu]/[Co] = 1.1. Hereinafter, the content is expressed in mass percent.

Target 1 was prepared by simultaneous ion deposition of cobalt and copper with two different ion beams on the nickel surface without subsequent annealing. This made it possible to obtain a deposited layer with a thickness of 760 nm at a metal content ratio according to the results of Energy Dispersive X-Ray (EDX) analysis [Cu]/[Co] = 1.34. The total foreign matter content was less than 10%, with more than half of this amount being carbon deposited for electron microscopy.

To prepare target 2, we used the method of layer-by-layer plasma sputtering on a nickel substrate. Figure 1 shows photographs of the surface of such a target and its cross section obtained by ion etching. Target 2 consists of 40 alternating layers of cobalt and copper with a total thickness of 1020 nm. The thickness of each monometallic layer in the target was 25–27 nm for cobalt and 27–31 nm for copper, and the ratio of the metal contents in the target was [Cu]/[Co] = 1.09.

The idea of forming bimetallic layers to obtain nanoparticles whose composition differs from the composition of solid solutions is generally not new and was used in one form or another in Refs [23, 24]. They show the fruitfulness of this method for creating heterometallic particles. However, this approach does not eliminate the main disadvantage of laser ablation in a liquid – a rather large spread in particle sizes.

The novelty in our case lies in the formation of these layers by the method of ion sputtering. This makes it possible to form layers with high accuracy, which, in turn, makes it possible to reliably determine the elemental composition of the resulting bimetallic nanoparticles.

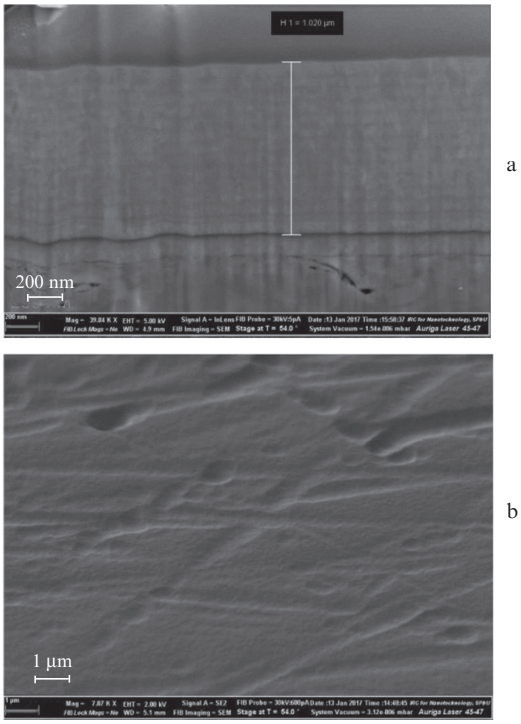


**Figure 1.** (a) Cross section and (b) surface of the layered structure of target 2 (layer-by-layer deposition). Element mass ratio is [Cu]/[Co] = 1.09.

The required layer thickness and the total thickness of the ablated target were calculated based on the parameters of an elementary ablation event. A necessary condition is the ablation of several layers from the target surface in a single ablation event. According to our estimates, the depth of ablation performed by one laser pulse is 60–65 nm.

### 3.2. Production of Co–Cu nanoparticles

As a result of the action of a laser pulse on a layered target, a shallow crater is formed (Fig. 2). The image of the crater and the micrograph of its bottom show a structure with a developed surface and a characteristic size of 1–3 μm, free from traces of melting or ejection of significant fragments. In Ref. [8], photographs of similar craters with the observed periodicity of the structure for bronze, brass and tungsten are presented.

After centrifugation of a colloidal solution of nanoparticles, their suspension was applied to a silicon substrate and dried. Elemental analysis showed that the [Cu]/[Co] content ratio for nanoparticles from the first target is 1.75, and from the second, 0.84. For further work, nanoparticles from the second target were selected, since the indicated ratio for them is closer to the previously selected value 1.1.

Figure 3a shows a micrograph of Co–Cu nanoparticles obtained by laser ablation, and Fig. 3b shows their size distribution.

Histograms were obtained using the Gatan Digital Micrograph and ImageJ software with correction for contrast and background brightness. The distribution diagrams were plotted with a change in the contrast and brightness of the micrograph to eliminate the effect of the background on the measurement results. Histograms were constructed by counting nanoparticles with pixel-sized calibration. Since the mea-

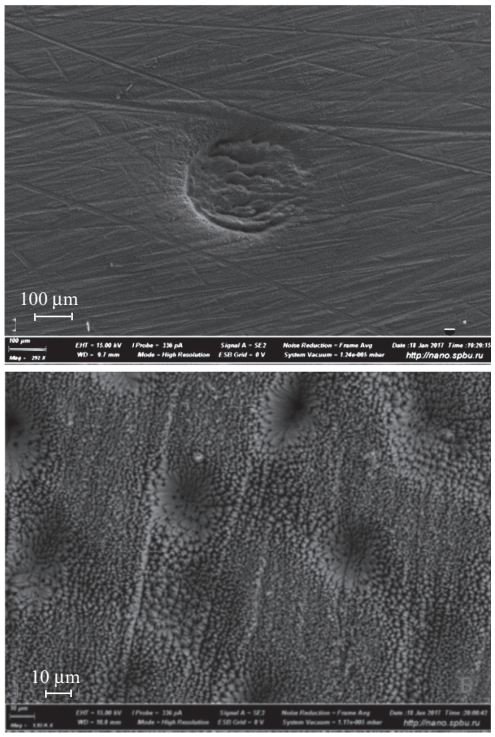


**Figure 2.** Images of an ablation crater on the surface of a Co–Cu target: (a) general view and (b) structure of the crater bottom.

surement results are highly dependent on the preparation of the image, the histograms were calculated manually from three photographs printed in A3 format with the maximum resolution. The histograms obtained by three methods coincide with an error of about 9%.

The average diameter of nanoparticles is $D = 33$ nm, and the half-width of their size distribution is $W = 12$ nm. However, there is a more adequate parameter $M$ characterising the degree of monodispersity of the ensemble, which is calculated as the ratio of the average diameter to the distribution half-width. For the ensemble under consideration, $M = 2.75$. Elemental analysis showed that the Ni content does not exceed 4%. This indicates that the thickness of the layered target is sufficient for practical elimination of the substrate ablation. A photograph of individual nanoparticles (Fig. 3a) shows that they have a regular spherical shape and, therefore, were formed directly during the ablation event rather than during the subsequent agglomeration.

The absence of traces of subsequent agglomeration, which can be expected for magnetic particles, is probably due to several reasons. First, the volume of these nanoparticles is one and a half orders of magnitude smaller than the volume of single-domain Co particles [25]. Second, magnetic particles are only half composed of Co, which, moreover, is a solid solution of copper in cobalt. As a result, the magnetism of the nanoparticles is apparently insufficient to lead to their agglomeration.

The following scheme was used to extract nanoparticles directly from the colloidal solution during laser ablation and fix them on the surface (Fig. 4). A polished silicon substrate was placed in the ablation cuvette perpendicular to the target. Part of its surface was coated with pure cobalt using vacuum deposition. The thickness of the cobalt coating was 860 nm (Fig. 5a demonstrates the quality of the applied cobalt layer). A permanent magnet was installed outside the cell so that its lines of force were perpendicular to the surface of the silicon substrate.

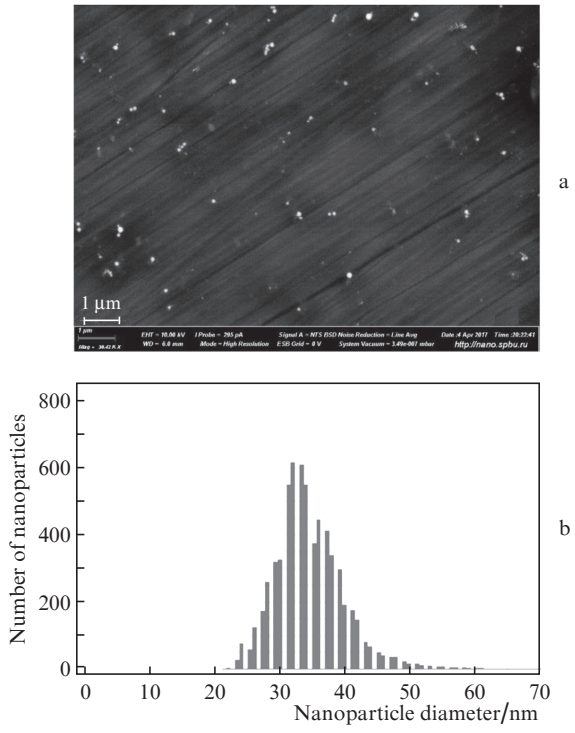


**Figure 3.** (a) Micrograph of Co–Cu nanoparticles obtained by laser ablation in liquid and (b) diagram of nanoparticle size distribution.

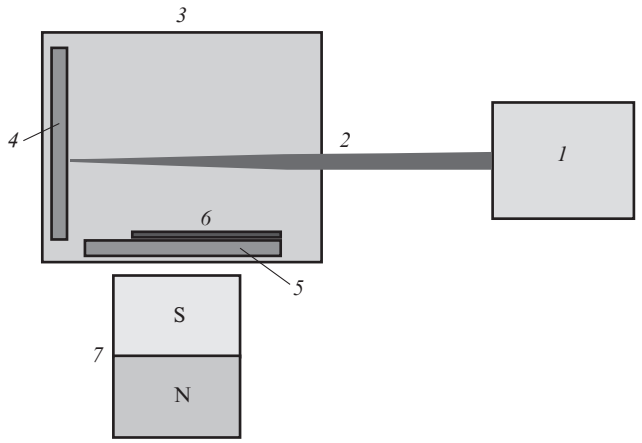


**Figure 4.** Schematic of the setup (side view) for ablation of a Co–Cu target in a magnetic field: (*1*) laser radiation source; (*2*) laser beam; (*3*) cell; (*4*) target; (*5*) silicon substrate; (*6*) deposited Co–Cu layer; (*7*) magnet.

Immediately after the ablation, the silicon substrate was removed from the cuvette without any additional operations. Figure 5b shows that a ferromagnetic cobalt film, in contrast to a clean surface of a silicon substrate, effectively retains Co–Cu nanoparticles obtained by laser ablation in a magnetic field. It should also be noted that, judging by the photograph (Fig. 5b), the ensemble of nanoparticles has a rather

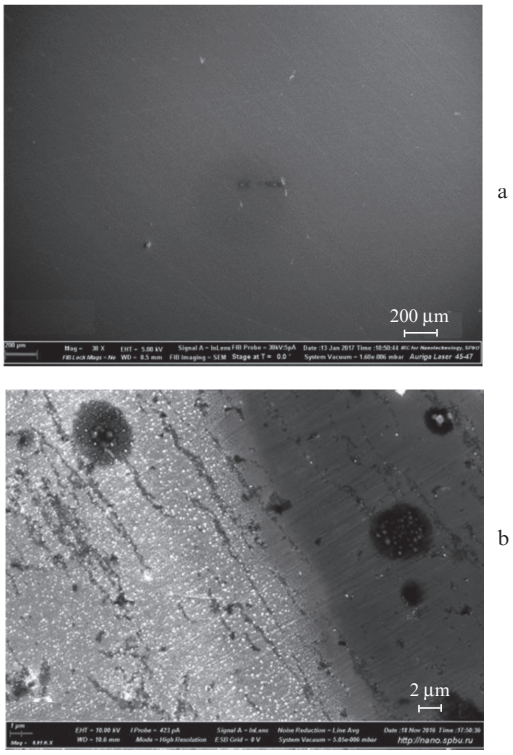


**Figure 5.** (a) Silicon substrate with a ferromagnetic cobalt layer before deposition of Co–Cu nanoparticles and (b) the boundary between the areas of the silicon substrate covered with a cobalt layer (left) and uncoated (right) after deposition of Co–Cu nanoparticles in a magnetic field; contrasting white inclusions are clearly visible, corresponding to deposited nanoparticles.

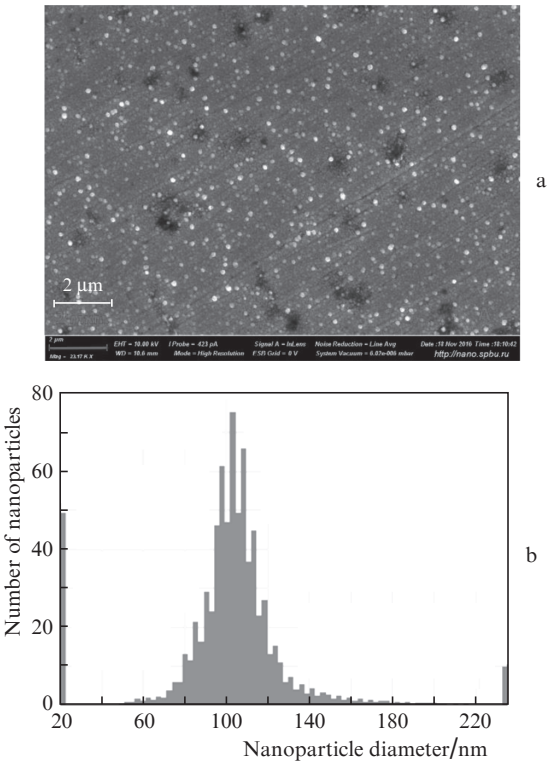


**Figure 6.** (a) Micrograph of Co–Cu nanoparticles obtained by laser ablation in a constant magnetic field and (b) diagram of nanoparticle size distribution.

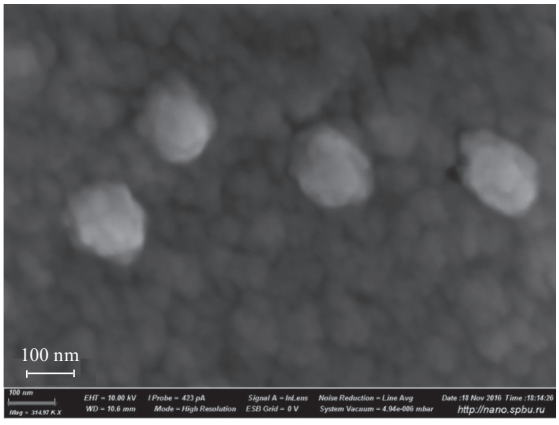


**Figure 7.** Micrograph of four Co–Cu nanoparticles. Their granular structure is visible.

narrow size distribution. This was confirmed by an analysis of the particle size distribution (Fig. 6b), performed using a photograph of an ensemble of nanoparticles located on a section of a silicon substrate covered with a cobalt layer (Fig. 6a).

It can be seen from Fig. 6b that the application of a magnetic field during ablation led to two significant changes in the parameters of the ensemble of the resulting nanoparticles. The average nanoparticle diameter $D$ increased by 3.5 times and became equal to 120 nm. This means that their volume has increased 40–50 times. The half-width of the nanoparticle size distribution $W$ was found to be 19 nm. Thus, the parameter $M$ increased by 2.3 times and reached a value of 6.3.

It can hardly be assumed that the magnetic field has a significant effect on the ablation process itself, characterised by high temperatures and energy consumption. Most likely, it stimulates the agglomeration of nanoparticles, increasing their initially insufficient magnetic moments. A photograph of individual nanoparticles (Fig. 7), which convincingly demonstrates that they are dense agglomerates of smaller nanoparticles confirms this.

Analysis of the literature data on the size distribution of nanoparticles [8, 21, 22, 25–27] shows that the degree of monodispersity is significant and cannot be a result of purely statistical processes. To achieve this, there must be a mechanism that increases the probability of the formation of medium-sized nanoparticles. It can be assumed that in this case such a mechanism is based on the achievement of the critical size of single-domain particles by nanoparticles as a result of the agglomeration process. It is known that it is precisely single-domain nanoparticles that have the maximum coercive force and magnetisation [25, 27]. According to [21], the critical size of single-domain particles of pure cobalt is 70 nm. It was shown in [18] that the coercive field for nanoparticles containing copper and cobalt with a concentration ratio of [Cu]/[Co] = 0.5 is only 3.2 times smaller than for nanoparticles of pure cobalt. In this regard, the assumption that the size of the Co–Cu nanoparticles obtained in a magnetic field, equal to 120 nm, is close to the critical size of single-domain nanoparticles with the ratio [Cu]/[Co] = 0.84, seems reasonable. Thus, the agglomeration of individual nanoparticles in an external magnetic field is apparently limited by the attainment of the critical size of single-domain particles. This explains the relatively narrow size distribution of agglomerated particles.

## 4. Conclusions

The use of a target consisting of alternating Co and Cu nanolayers makes it possible to obtain intermetallic nanoparticles with a composition close to the specified one by laser ablation in a liquid. Ablation in a magnetic field makes it possible to increase the monodispersity of the ensemble of the resulting nanoparticles. The half-width of the nanoparticle size distribution turns out to be less than the average nanoparticle size by more than six times. The possibility of efficient extraction of ferromagnetic nanoparticles from a colloidal solution in which ablation was carried out using a substrate coated with a cobalt film less than a micrometer thick in an applied constant magnetic field is shown. The unification of the size of cobalt nanoparticles is important when they are used in heterogeneous catalysis, including in closed-type reactors, where the catalyst is obtained by laser ablation directly in the reaction medium.

***Acknowledgements.*** The measurements were performed in the resource centres of the Research Park of St. Petersburg State University: Centre for Optical and Laser Materials Research, Interdisciplinary Resource Centre for Nanotechnology, Centre for Physical Methods of Surface Investigation, Centre for Geo-Environmental Research and Modelling (GEOMODEL).

## References

1. Devarajan S., Bera P., Sampath S. *J. Colloid Interface Sci*., **290**, 117 (2005).
2. Cheng Y., Yu G., Tang L., Zhou Y., Zhang G. *J. Crystal Growth*, **334** (1), 181 (2011).
3. Chenga J., Bordes R., Olssonb E., Holmberga K. *Colloids Surf. A: Physicochem. Eng. Aspects*, **436** (5), 823 (2013).
4. Sakai K., Kingetsu T. *J. Crystal Growth*, **126** (2-3), 184 (1993).
5. Iijima Y., Takahashi Y., Matsumoto K., Hayashi T., Todoroki N., Wadayama T. *J. Electroanal. Chem*., **685**, 79 (2012).
6. Shatrova N., Yudin A., Levina V., Dzidziguri E., Kuznetsov D., Perov N. *Mater. Res. Bull*., **86**, 80 (2017).
7. Aliofkhazraei M., Ali N., in *Comprehensive Materials Processing* (2014) Vol. 7, P. 7.05.6, pp 85–117.
8. Kazakevich P.V., Simakin A.V., Shafeev G.A. *Appl. Surf. Sci*., **252**, 4457 (2006).
9. Kazakevich P.V., Voronov V.V., Simakin A.V., Shafeev G.A. *Quantum Electron*., **34** (10), 951 (2004) [*Kvantovaya Elektron*., **34** (10), 951 (2004)].
10. Goncharova D.A., Lapin I.N., Savelyev E.S., Svetlichnyi V.A. *Russ. Phys. J*., **60** (7), 1197 (2017) [*Izv. Vyssh. Uchebn. Zaved., Ser. Fiz.*, **60** (7), 98 (2017)].
11. Qiao X., Wie X., Hao Y., Zhang Y., Xu M., Ye B. *Mater. Lett*., **236**, 46 (2019).
12. Patel P., Nandi S., Maru M.S., Kureshy R.I., Khan N.-ul H. *J. $CO_2$ Utilization*, **25**, 310 (2018).
13. Zhang X.-F., Meng H.-B., Chen H.Y., Feng J.J., Fang K.M., Wang A.J. *J. Alloys Compounds*, **786**, 232 (2019).
14. Sravani B., Raghavendra P., Chandrasekhar Y., Reddy Y.V.M., Sivasubramanian R., Venkateswarlu K., Madhavi G., Subramanyam S.L. *Int. J. Hydrogen Energy*, **45** (13), 7680 (2020).
15. Pu Y., Tao X., Zeng X., Le Y., Chen J.-F. *J. Magnetism Magnetic Mater*., **322** (14), 1985 (2010).
16. Wen M., Liu Q.-Y., Wang Y., Zhu Y.-Z., Wu Q.-S. *Colloids Surf. A: Physicochem. Eng. Aspects*, **318** (1-3), 238 (2008).
17. Wu D., Yuan J., Yang B., Chen H. *Surf. Sci.*, **671**, 36 (2018).
18. Fernandez C.J., Mattei G., Maurizio C., Cattaruzza E., Padovani S., Battaglin G., Gonella F., D'Acapito F., Mazzoldi P. *J. Magnetism Magnetic Mater*., **290-291**, 187 (2005).
19. Kim J.D., Petford-Long A.K., Jakubovics J.P., Evetts J.E., Somekh R. *J. Appl. Phys*., **76**, 2387 (1994).
20. Svetlichnyi V.A., Balashov V.B., Lapin I.N., Cherepanov V.N., Sokolov A.E. *Russ. Phys. J.*, **62** (3) 411 (2019) [*Izv. Vyssh. Uchebn. Zaved., Ser. Fiz*., **62** (3), 26 (2019)].
21. Chernavsky S.A. Ross. *Khim. Zh*., **XLVI** (3), 19 (2002).
22. Liu G., Niu T., Pan D., Liu F., Liu Y. *Appl. Catalysis A: General*, **483**, 10 (2014).
23. Oh Y., Lee J., Lee M. *Appl. Surf. Sci.*, **434**, 1293 (2018).
24. Sachan R., Yadavali S., Shirato N., Krishna H., Ramos V., Duscher G., Pennycook S.J., Gangopadhyay A.K., Garcia H., Kalyanaraman R. *Nanotechnology*, **23** (27), 1 (2012).
25. Meng H., Zhao F., Zhang Z. *Int. J. Refractory Metals Hard Mater.*, **31**, 224 (2012).
26. Frolov G.I., Bachina O.I., Zavyalova M.M., Ravochkin S.I. *Techn. Phys*., **53**, 1059 (2008) [*Zh. Tekhn. Fiz*., **78**, 101 (2008)].
27. Zhang J., Lan C.Q. *Mater. Lett*., **62** (10-11), 1521 (2008).